



<https://doi.org/10.5281/zenodo.15695590>

Integration of Motor-Assisted Planetary CVT Systems for Wind Turbines under Variable Wind Conditions

1st Kamaliddin Abdivakhidov

Kimyo International University in Tashkent
Tashkent, Uzbekistan
kamol.abdivakhidov@gmail.com

2nd Malika Platoshina

Kimyo International University in Tashkent
Tashkent, Uzbekistan
malika.malich.dzhalilova@gmail.com

Abstract – This paper presents a novel continuously variable transmission (CVT) system for wind turbine applications, combining a planetary gearbox with a motor-assisted control mechanism. The proposed architecture enables real-time adjustment of the transmission ratio by dynamically regulating the ring gear using a synchronous electric motor. A detailed mathematical model is developed to describe the gear kinematics and torque distribution, followed by a complete Simulink implementation that captures the electromechanical interactions between the turbine input, planetary gear system, and motor controller. Simulations were conducted for three motor speed scenarios (600, 1200, and 1800 rpm), representing low, medium, and high wind conditions. The results confirm the system’s ability to stabilize torque, adapt output speed, and respond effectively to dynamic changes in input conditions. The integration of electric motor control within a planetary CVT system offers improved flexibility, efficiency, and control precision for variable-speed wind turbine applications.

Index Terms – Continuously Variable Transmission (CVT), Planetary Gearbox, Wind Turbine, Motor-Assisted Control, Simulink Modeling, Transmission Ratio, Electromechanical Simulation.

I. INTRODUCTION

The ongoing global transition toward renewable energy sources has intensified the demand for more efficient and adaptive wind turbine technologies. Despite significant advancements in generator efficiency, blade aerodynamics, and power electronics, the mechanical drivetrain remains a limiting factor in the overall performance of wind energy systems. Most commercial wind turbines utilize

fixed-ratio gearboxes that are designed for optimal efficiency at a narrow range of wind speeds. When real wind conditions deviate from this nominal operating point, these systems suffer from torque mismatch, increased stress, and reduced energy conversion efficiency [2], [7].

To address this, continuously variable transmission (CVT) systems have been explored as a way to dynamically adjust the transmission ratio and maintain optimal shaft speed under variable wind conditions. However, conventional CVT designs – such as belt-driven or toroidal systems – are typically limited in torque capacity and durability, making them unsuitable for large-scale wind turbine applications [3], [11]. Furthermore, these systems often lack precise real-time controllability when faced with stochastic wind inputs.

Planetary gear systems have been extensively studied for their compactness, torque density, and ability to distribute mechanical load. Their inherent structure enables variable transmission when integrated with a controllable element such as an auxiliary electric motor. By connecting a motor to the ring gear and actively controlling its speed or torque, the overall gear ratio can be varied in real time, allowing for smooth and adaptive operation [1], [6], [14]. This motor-assisted planetary CVT concept has demonstrated potential in improving efficiency and reducing mechanical wear in systems subjected to highly variable inputs [10], [13].

While prior research has validated the theoretical feasibility of such systems in automotive and industrial contexts, their integration into wind turbine drivetrains remains largely unexplored. Few simulation studies consider the full electromechanical coupling between wind rotor dynamics, CVT mechanisms, and motor control systems [4], [15]. In addition, existing work often lacks comparative analysis across different wind speed regimes.

$$\frac{\partial C}{\partial t} = D \frac{\partial^2 C}{\partial x^2} \quad (1)$$

In equation 1, C is the corrosive agent concentration within the coating, t is time, D is the diffusion coefficient (which is determined by the coating material's properties), and x is the distance from the surface. Fick's Law describes how the diffusivity and thickness of a coating influence the rate at which a corrosive agent penetrates it. Coatings with low diffusion coefficients and increased thickness are more resistant to corrosive penetration, providing better long-term protection.

In addition to diffusion control, a coating's adhesion strength is critical for its continued effectiveness. A thinly adhered coating can delaminate under mechanical or thermal stress, exposing the underlying metal to corrosive elements. The adhesive strength can be calculated using fracture mechanics, in which the energy release rate quantifies the work required to propagate a crack between the coating and the substrate. This concept can be expressed through Griffith's energy criterion for fracture [3]:

$$G = \frac{\sigma^2 h}{E} \quad (2)$$

Here, G is the energy release rate, σ is applied stress, h is the coating thickness, and E is the material's elastic modulus. The higher the energy release rate, the more resistant the coating is to delamination, resulting in improved protection over time.

Coating technologies have evolved beyond standard protective approaches to incorporate functional features that enhance performance. Thermal spray coatings, for example, offer greater corrosion, wear, and heat resistance by spraying molten materials onto a substrate. These coatings are commonly utilized in applications involving intense mechanical and thermal loads, such as turbines, exhaust systems, and marine vessels. Thermal spray coatings, which deposit materials such as ceramics, composites, or metal alloys, provide a robust barrier that considerably improves the service life of metal components [4].

Similarly, nanocomposite coatings have gained popularity because of their superior mechanical and chemical properties. Coatings that incorporate nanoparticles like TiO₂, SiO₂, or carbon nanotubes into a polymer or ceramic matrix improve the protective layer's toughness, hardness, and chemical resistance. Nanoparticles have a high surface area-to-volume ratio, which promotes interaction with the matrix and results in more stable and durable coatings. Furthermore, nanocomposite coatings frequently exhibit self-healing properties, in which microcapsules embedded within the coating release healing agents when damaged, autonomously repairing minor cracks or defects before they spread and compromise the metal substrate.

The next frontier in protective coatings is smart coatings, which respond to changes in the environment and adjust their properties accordingly. Some smart coatings, for example, employ stimuli-responsive polymers that respond to changes in temperature, pH, or moisture content. In corrosive conditions, these coatings can alter their permeability or surface energy to decrease exposure to corrosive materials. Smart coatings give an extra layer of protection by dynamically altering their properties in response to environmental changes. Industries such as oil and gas, where environmental conditions can change rapidly, have begun to use smart coatings to protect pipelines and drilling platforms from corrosion.

Finally, the development of advanced coatings is critical for protecting metal structures against corrosion. While traditional coatings provide basic protection, contemporary coating technologies, such as nanocomposites and thermal sprays, as well as smart coatings, improve functionality, durability, and environmental responsiveness. As industries operate in more severe conditions, the demand for high-performance protective coatings will only grow. This review will look at advanced metal coating technologies, highlighting their applications, performance characteristics, and the benefits they provide in terms of corrosion protection and longer service life.

II. LITERATURE REVIEW

The efficiency and adaptability of wind turbine drivetrains remain a persistent challenge, particularly in environments characterized by fluctuating wind speeds. Traditional systems based on fixed-ratio gearboxes are mechanically robust but fail to provide the necessary flexibility under non-nominal conditions. As a result, wind turbines operate inefficiently for a large portion of their active lifetime, with performance degradation attributed to torque mismatch and speed imbalance [2], [7].

Efforts to overcome these limitations have led to the investigation of continuously variable transmission (CVT) mechanisms. Early implementations such as belt-based and toroidal CVTs demonstrated smooth ratio transitions, yet were limited by their torque capacity and high susceptibility to wear under oscillatory load profiles [3], [11]. Consequently, such designs remain impractical for utility-scale wind turbines.

To improve adaptability while maintaining torque-handling capacity, researchers have proposed integrating planetary gear sets into CVT architectures. Planetary systems offer compact, high-torque configurations and enable continuous ratio modulation when one of the gear components – typically the ring gear – is controlled externally. The fundamental relationship among the angular velocities of the sun gear (ω_s), carrier (ω_c), and ring gear (ω_r) in a simple planetary gear set is given by:

$$\frac{\omega_c - \omega_r}{\omega_s - \omega_r} = \frac{R_s}{R_r} \quad (3)$$

where R_s and R_r are the radii (or number of teeth) of the sun and ring gears, respectively [1], [6].

This kinematic relationship allows modulation of the output speed by controlling the ring gear's motion. By coupling a controllable electric motor to the ring gear, one can actively influence ω_r , thereby varying the transmission ratio in real time:

$$i(t) = \frac{\omega_s(t) - \omega_r(t)}{\omega_c(t)} \quad (4)$$

where $i(t)$ is the instantaneous gear ratio [10], [14].

Yao and Lin [14] proposed such a motor-assisted planetary CVT system, in which a permanent magnet synchronous motor (PMSM) interacts with the planetary gear train. Their model demonstrated that motor torque can effectively regulate gear ratio and stabilize output speed under variable input conditions. Sun et al. [10] extended this concept by integrating a real-time feedback control system, utilizing inverter-fed motors and sensor-driven control loops.

Despite theoretical advances, full electromechanical modeling of such systems in wind turbine applications remains sparse. Bilal et al. [3] introduced a novel CAD CVT configuration optimized for mechanical integration, yet it lacked an active control strategy. Boutahiri et al. [4] modeled turbine behavior using a DC motor emulator, without incorporating planetary mechanics. Similarly, Yin and Jiang [15] presented a magnetorheological (MR) transmission system for offshore turbines that focused on vibration damping, not ratio modulation.

Control-oriented studies, such as those by Xin et al. [13], investigated receding horizon control for energy efficiency in logistics, suggesting that predictive algorithms could also be adapted for drivetrain optimization. However, no comprehensive study currently combines planetary mechanics, real time motor control, and wind speed variability in a unified simulation framework.

This gap motivates the present research, which develops and evaluates a motor-assisted planetary CVT system using a dynamic model in MATLAB/Simulink. The model includes detailed gear interactions, motor dynamics, and closed loop control strategies, all tested across realistic wind-driven operating conditions.

III. MOTOR-ASSISTED PLANETARY CVT SYSTEM

The proposed continuously variable transmission (CVT) system integrates a planetary gear set with a controllable synchronous electric motor. This combination enables real-time adjustment of the transmission ratio to accommodate variable wind conditions and maintain stable output torque and speed. The core idea is to exploit the mechanical properties of a planetary gearbox while dynamically regulating one of its components – the ring gear – using a closed loop motor control system.

A. System Architecture and Operating Principle

As illustrated in Fig. 1, the CVT system receives mechanical input from the wind turbine, which drives the sun gear of a planetary gear set. The output is extracted from the carrier, and the ring gear is connected to a synchronous electric motor. The motor torque is modulated based on a feedback control algorithm that reacts to load conditions and shaft speed deviations.

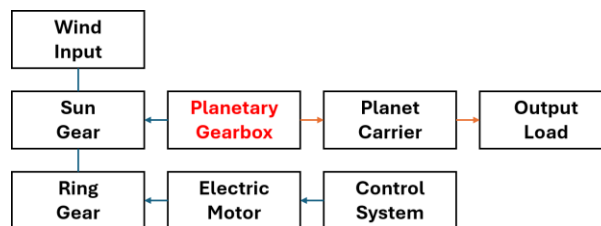


Fig. 1. Architecture of the motor-assisted planetary CVT system. Wind input drives the sun gear; the synchronous motor controls the ring gear to modulate the transmission ratio through the planetary carrier.

This configuration allows the transmission ratio $i(t)$ to be adjusted continuously by changing the angular velocity of the ring gear $\omega_r(t)$. The angular velocity of the carrier $\omega_c(t)$, which determines the output shaft speed, is given by the kinematic relation:

$$\omega_c(t) = \omega_r(t) + \left(\frac{R_s}{R_r}\right) [\omega_s(t) - \omega_r(t)] \quad (5)$$

where $\omega_s(t)$ is the sun gear speed (input), and R_s, R_r are the radii (or number of teeth) of the sun and ring gears respectively. The dynamic transmission ratio can be expressed as:

$$i(t) = \frac{\omega_s(t) - \omega_r(t)}{\omega_c(t)} \quad (6)$$

The system operates in three modes depending on the electric motor control:

1. *Passive mode* – motor is unpowered; ring gear is free- floating.
2. *Assistive mode* – motor provides compensating torque to stabilize speed.
3. *Active mode* – motor fully controls ring gear speed based on feedback.

B. Material Considerations for Mechanical Components

The gear components in the planetary system are subjected to cyclic loading and continuous rotational contact. For this reason, the choice of gear material and its heat treatment are relevant to the long-term mechanical behavior of the system. Previous investigations [20] have examined how quenching and tempering affect the structure of steels under thermal treatment and surface modification, which may inform material selection strategies for planetary systems exposed to variable-speed operation.

The use of combined chemical-thermal treatments has also been explored in other studies [21], providing additional insights into how the microstructure of high-speed steels can be modified to suit specific operating environments in rotating systems.

Moreover, in mechanical systems where contact surfaces are exposed to outdoor environments, surface protection may be considered to reduce material degradation over time. Prior studies have addressed this topic in the context of metallic coatings for rotating elements [17].

IV. SIMULATION MODEL AND METHODOLOGY

Model-based approaches have been applied in many engineering domains to assess system response without requiring physical prototypes. This strategy has also been used in studies involving geomechanical processes [19], and is followed here to simulate the electromechanical behavior of the CVT system. To validate the dynamic performance of the proposed CVT system, a detailed electromechanical model was developed in MATLAB/Simulink using Simscape Multibody and Simscape Electrical libraries. The model reflects the physical behavior of the main drivetrain components and enables closed loop control of the ring gear via an electric motor.

A. Overall System Structure

The complete model is illustrated in Fig. 2. It consists of four interconnected subsystems:

1) **Wind Input Subsystem** – delivers mechanical torque and angular speed to the sun gear of the planetary gearbox. This block emulates the aerodynamic torque generated by wind forces acting on a turbine rotor.

2) **Planetary Gearbox Subsystem** – based on the topology shown in Fig. 1, this subsystem includes sun (S), ring (R), and carrier (C) ports. The gear kinematics follow the planetary relationship described in Eq. (3) of Section 3:

$$\omega_c(t) = \omega_r(t) + \left(\frac{R_s}{R_r}\right) [\omega_s(t) - \omega_r(t)] \quad (7)$$

In the Simulink model, these mechanical ports are connected using Simscape rotational interfaces, ensuring that power, torque, and speed are conserved throughout the transmission path.

Electric Motor and Control Subsystem – a three-phase permanent magnet synchronous motor (PMSM) is connected to the ring gear. It is driven by a voltage source inverter, whose gating signals are generated by a PID-based control system. The motor's torque directly controls the ring gear velocity $\omega_r(t)$, and hence the instantaneous transmission ratio $i(t)$ defined earlier:

$$i(t) = \frac{\omega_s(t) - \omega_r(t)}{\omega_c(t)}$$

The motor operates in torque-control mode, where the inverter modulates three phase voltages to achieve desired angular velocity. The controller aims to minimize the tracking error:

$$e(t) = \omega_{ref}(t) - \omega_c(t)$$

and computes the control law via:

$$u(t) = K_p e(t) + K_I \int e(t) dt + K_D \frac{de(t)}{dt}$$

3) **Load Subsystem** – models the resistive and inertial characteristics of a generator or mechanical load. It is connected to the carrier of the planetary gear and responds to the net torque delivered by the CVT system. Its load resistance can be varied parametrically to test different operating points.

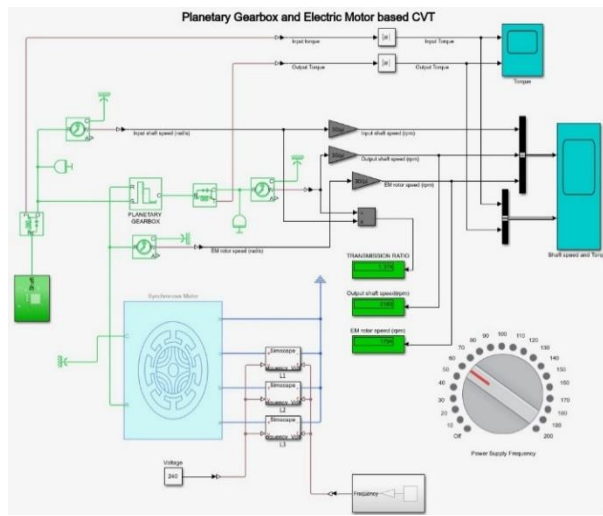


Fig. 2. Complete Simulink implementation of the CVT system, including planetary gearbox, synchronous motor, inverter, PID control system, and measurement blocks.

B. Simulation Parameters and Environment

All simulations were run using the Variable-Step Solver in Simulink with a maximum step size of 0.001 s. Key system parameters include:

- Gear tooth ratio: $\frac{R_s}{R_r} = 0.45$
- Motor nominal speed: 1800 rpm
- Rated torque (motor): 35 Nm
- Load inertia: $0.03 \text{ kg}\cdot\text{m}^2$
- Shaft stiffness: 800 Nm/rad
- Control sample time: 1 ms

Measurement blocks are placed at all shaft interfaces to monitor torque, angular velocity, and computed transmission ratios in real time. The transmission ratio is calculated using speed signals from the planetary ports, based on Eq. (4).

C. Simulation Scenarios

To analyze the system's performance across a realistic wind spectrum, three scenarios were executed, each corresponding to a fixed motor rotor speed:

- **Low-speed mode** – EM rotor set to 600 rpm

- **Mid-speed mode** – EM rotor set to 1200 rpm
- **High-speed mode** – EM rotor set to 1800 rpm

Each scenario was simulated over 8 seconds to capture transient and steady-state behavior. Output data includes torque waveforms, shaft speeds, and CVT transmission ratios under varying load conditions.

V. RESULTS AND DISCUSSION

The simulation results provide insights into the dynamic response of the proposed CVT system under various motor rotor speeds. The main outputs analyzed are input/output shaft speeds, motor rotor speed, and corresponding torque profiles. Transmission ratio adaptation is also tracked in each case to evaluate responsiveness and control stability.

A. Case 1: EM Rotor Speed = 600 rpm

Figure 3 shows the system behavior when the motor rotor speed is maintained at 600 rpm. The input shaft (sun gear) speed remains at approximately 3000 rpm, while the output carrier stabilizes near 1376 rpm. The low rotor speed results in a relatively high transmission ratio:

$$i(t) = \frac{3000 - 600}{1376} \approx 2.18.$$

The torque signals indicate oscillations at the output as the control system responds to wind input variations. Output torque is amplified due to the mechanical advantage provided by the gear train.

B. Case 2: EM Rotor Speed = 1200 rpm

In this scenario (Fig. 4), the motor rotor speed is increased to 1200 rpm. The output shaft stabilizes near 1785 rpm, and the transmission ratio is reduced accordingly:

$$i(t) = \frac{3000 - 1200}{1785} \approx 1.68.$$

Compared to Case 1, the system demonstrates smoother torque dynamics and faster response. Output speed increases while torque multiplication decreases, as expected.

C. Case 3: EM Rotor Speed = 1800 rpm

Figure 5 shows the results for the highest motor speed scenario. The motor rotates at 1800 rpm, and the output shaft reaches approximately 2193 rpm. The transmission ratio decreases further:

$$i(t) = \frac{3000 - 1800}{2193} \approx 1.37.$$

This configuration prioritizes speed over torque, suitable for low-load, high-wind conditions. The control system maintains high tracking precision, as evidenced by minimal difference between input and output torque signals.

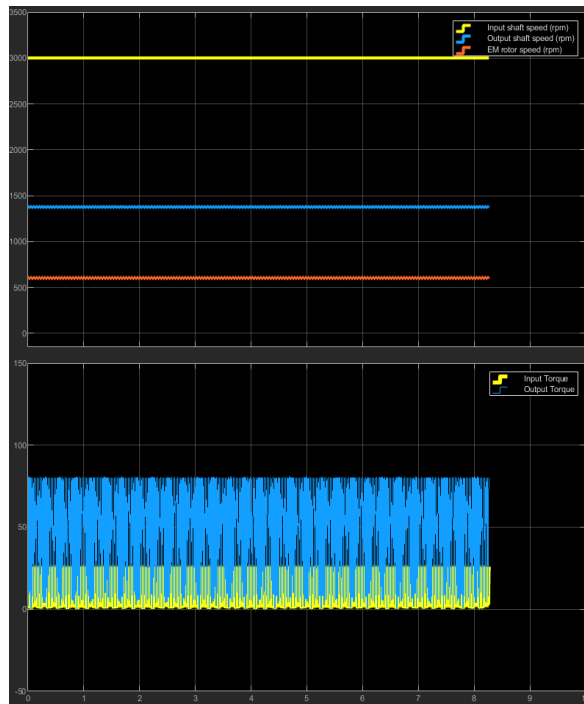


Fig. 3. Simulation results at EM rotor speed = 600 rpm. Top: shaft speeds (rpm). Bottom: input/output torque (Nm).

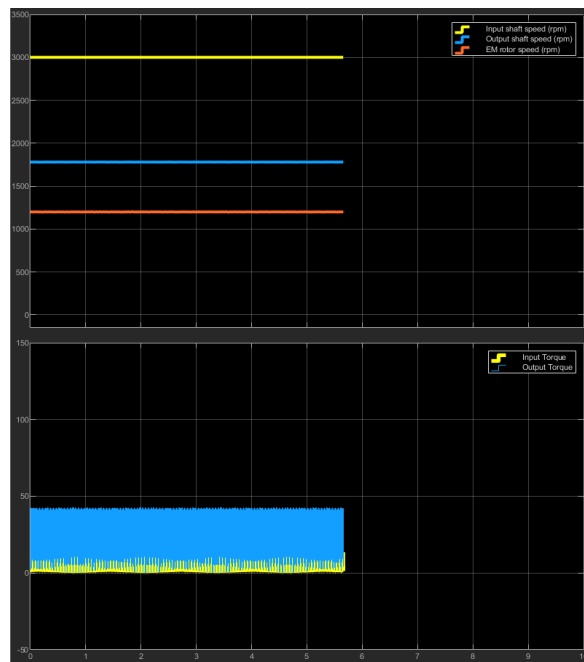


Fig. 4. Simulation results at EM rotor speed = 1200 rpm. Top: shaft speeds (rpm). Bottom: input/output torque (Nm).

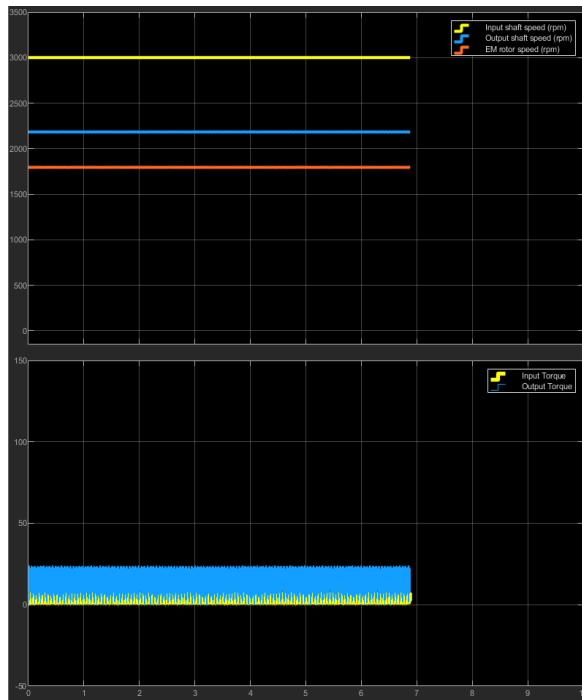


Fig. 5. Simulation results at EM rotor speed = 1800 rpm. Top: shaft speeds (rpm). Bottom: input/output torque (Nm).

TABLE I

TRANSMISSION RATIO AND OUTPUT SPEED AT DIFFERENT MOTOR SPEEDS

EM Rotor Speed (rpm)	Ratio $i(t)$	Output Shaft Speed (rpm)
600	2.18	1376
1200	1.68	1785
1800	1.37	2193

D. Comparative Analysis

Figure 6 presents a comparison of output shaft speeds across the three cases. The EM rotor speeds of 600, 1200, and 1800 rpm show progressively increasing output speeds and decreasing transmission ratios. These data confirm that the control system effectively modulates ring gear speed to meet varying transmission demands in real time.

Table I summarizes the steady-state transmission ratios and output shaft speeds for each scenario. As motor speed increases, the transmission ratio $i(t)$ decreases, which in turn raises output speed but reduces torque multiplication.

VI. CONCLUSION

This study proposed and validated a motor-assisted planetary CVT (Continuously Variable Transmission) system designed for wind turbine applications. The concept integrates a planetary gear train with a synchronous electric motor connected to the ring gear, allowing for real-time modulation of the transmission ratio through a closed loop control system. The theoretical framework was supported by detailed mathematical modeling, which established the relationships among gear speeds, motor torque, and transmission behavior. The Simulink implementation provided a realistic environment to analyze system performance under varying wind conditions, represented by three

rotor speed scenarios (600, 1200, and 1800 rpm).

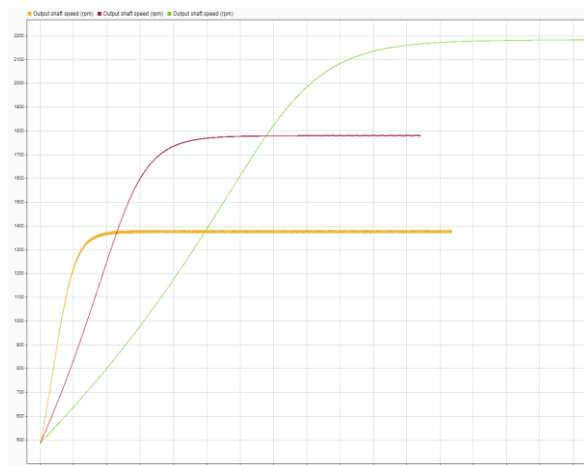


Fig. 6. Comparison of output shaft speed in three CVT configurations: EM rotor = 600, 1200, 1800 rpm. Extracted using Simulink Data Inspector.

Simulation results demonstrated the ability of the proposed system to:

- maintain stable output torque across a wide range of input conditions;
- dynamically adjust the transmission ratio in real time, with values ranging from 2.18 to 1.37;
- deliver increasing output shaft speeds as the motor rotor speed increased, validating the concept of active speed modulation;
- ensure control stability and responsiveness using a PID- based motor control loop.

For real-world applications, measures such as protective coatings can be included in system design to reduce the effects of moisture, dust, or temperature. A review of corrosion-resistant coating methods is provided in [18], including solutions applicable to gear housing and motor surfaces.

Overall, the integration of electric motor assistance with planetary gear mechanisms proves to be an effective approach to improving drivetrain flexibility and efficiency in wind energy systems. The model provides a solid foundation for future optimization, experimental validation, and hardware-in-the-loop implementation.

REFERENCES

- [1] Azzouz, M. S., Fagbe, A., Evetts, Z., & Rosales, E. (2012). Active conical and planetary gearing system for wind turbines. In *ASME 2012 International Mechanical Engineering Congress and Exposition* (pp. 1665–1674). <https://doi.org/10.1115/IMECE2012-86430>
- [2] Bekirov, E. A., Voskresenskaya, S. N., Ramazanova, Z. U., & Bekirov, O. S. (2024). Methods of calculating electric power generation by wind turbines and their influence on wind speed. *Power Engineering Research Equipment Technology*, 25(5), 30–41. <https://doi.org/10.30724/1998-9903-2023-25-5-30-41>
- [3] Bilal, M., Zhu, Q., Qureshi, S. R., Elahi, A., Nadeem, M. K., & Khan, S. (2024). A novel continuously variable transmission with circumferentially arranged disks (CAD CVT). *Actuators*, 13(6), 208. <https://doi.org/10.3390/act13060208>
- [4] Boutahiri, C., Nouaiti, A., Bouazi, A., & Hsaini, A. M. (2023). Wind turbine emulator based on DC motor. In *Advances in Systems Analysis, Software Engineering, and High-Performance Computing* (pp. 1–14). <https://doi.org/10.4018/979-8-3693-0497-6.ch001>
- [5] Dose, B., Rahimi, H., Herra'ez, I., Stoevesandt, B., & Peinke, J. (2018). Fluid-structure coupled computations of the NREL 5 MW wind turbine by means of CFD. *Renewable Energy*, 129, 591–605. <https://doi.org/10.1016/j.renene.2018.05.064>
- [6] Mangialardi, L., & Mantriota, G. (1996). Dynamic behavior of wind power systems equipped with automatically regulated continuously variable transmission. *Renewable Energy*, 7(2), 185–

203. [https://doi.org/10.1016/0960-1481\(95\)00125-5](https://doi.org/10.1016/0960-1481(95)00125-5)

- [7] Rex, A. H., & Johnson, K. E. (2009). Methods for controlling a wind turbine system with a continuously variable transmission in region 2. *Journal of Solar Energy Engineering*, 131(3). <https://doi.org/10.1115/1.3139145>
- [8] Rossi, C., Corbelli, P., & Grandi, G. (2009). W-CVT continuously variable transmission for wind energy conversion system. In *2009 IEEE Power Electronics and Motion Control Conference (PEMC)*, 1–10. <https://doi.org/10.1109/PEMWA.2009.5208399>
- [9] Siddiqui, O., & Dincer, I. (2019). Design and analysis of a novel solar-wind based integrated energy system utilizing ammonia for energy storage. *Energy Conversion and Management*, 195, 866–884. <https://doi.org/10.1016/j.enconman.2019.05.001>
- [10] Sun, X., Cheng, M., Zhu, Y., & Xu, L. (2013). Application of electrical variable transmission in wind power generation system. *IEEE Transactions on Industry Applications*, 49(3), 1299–1307. <https://doi.org/10.1109/TIA.2013.2253079>
- [11] Upadhyay, P., Pandey, S., Saxena, R., Dixit, Y., Yadav, V., Bansal, P., & Sharma, S. (2021). Investigating CVT as a transmission system prospect for wind turbine. In *Lecture Notes in Mechanical Engineering* (pp. 483–488). <https://doi.org/10.1007/978-981-33-4684-049>
- [12] Wu, X., Ma, Z., Rui, X., Yin, W., Zhang, M., & Ji, K. (2016). Speed control for the continuously variable transmission in wind turbines under sub synchronous resonance. *Iranian Journal of Science and Technology, Transactions of Mechanical Engineering*, 40(2), 151–154. <https://doi.org/10.1007/s40997-016-0007-7>
- [13] Xin, J., Negenborn, R. R., & Lodewijks, G. (2015). Event-driven receding horizon control for energy-efficient container handling. *Control Engineering Practice*, 39, 45–55. <https://doi.org/10.1016/j.conengprac.2015.01.005>
- [14] Yao, W., & Lin, C. (2022). Design of active continuous variable transmission control system with planetary gear. *Electronics*, 11(7), 986. <https://doi.org/10.3390/electronics11070986>
- [15] Yin, X., & Jiang, Z. (2023). A novel continuously variable-speed offshore wind turbine with magnetorheological transmission for optimal power extraction. *Energy Sources Part A: Recovery, Utilization, and Environmental Effects*, 45(3), 6869–6884. <https://doi.org/10.1080/15567036.2023.2217145>
- [16] Zhang, B., Chen, Y., Zhang, B., Peng, R., Lu, Q., Yan, W., Yu, B., Liu, F., & Zhang, J. (2021). Cyclic performance of coke oven gas-steam reforming with assistance of steel slag derivatives for high purity hydrogen production. *Renewable Energy*, 184, 592–603. <https://doi.org/10.1016/j.renene.2021.11.123>
- [17] Abdivakhidov, K. (2023). Application and removing protective metal coatings. *AIP Conference Proceedings*, 2789, 040087. <https://doi.org/10.1063/5.0149617>
- [18] Abdivakhidov, K., & Sharipov, K. (2024). Corrosion-resistant protective coatings for metals: A review of metallic and non-metallic coatings. *AIP Conference Proceedings*, 3045, 060011. <https://doi.org/10.1063/5.0197373>
- [19] Khudaykulov, S., Kodirov, D., Sherbaev, I., Musurmonov, M., & Abdivakhidov, K. (2023). Modeling determination of landslide pressure of Akhangaran reservoir ground masses. *E3S Web of Conferences*, 401, 02027. <https://doi.org/10.1051/e3sconf/202340102027>
- [20] B. J. Mukhammadjonovich, “Effect of Quenching and Tempering Temperatures on the Structure Formation of 4XMFC, 4X5MF1C Steels during Low Temperature Nitro-Cementation,” *International Journal of Mechatronics & Applied Mechanics*, no. 13, 2023
- [21] B. J. Mukhammadjonovich, “Influence of Combined Chemical-Thermal Treatment Modes on Structure Formation of High-Speed Steel,” *International Journal of Mechatronics & Applied Mechanics*, no. 14, 2023